J. Jpn. Soc. Powder Powder Metallurgy, **72** (2025) S555-S562
https://doi.org/10.2497/jjspm.15C-T1-21
©2025 Japan Society of Powder and Powder Metallurgy

Characterization of the Chemistry of Oxides formed on the Surface of Water-atomized Steel Particles during Annealing

Gabrielle LARAMÉE[1], Simon GÉLINAS[1], Philippe PLAMONDON[2], Jean-Philippe MASSE[2], Gilles L'ESPÉRANCE[2] and Carl BLAIS[1*]

[1]Université Laval, 2325 Rue de l'Université, Ville de Québec, G1V 0A6, Canada.
[2]Centre for Characterization and Microscopy of Materials (CM)[2], 2500 Chemin de Polytechnique, Montréal, QC H3T 1J4, Canada.

Abstract

Water-atomized (WA) steel powders are inevitably oxidized due to the chemical reaction between molten metal and water vapor. Minimization of surface oxides is essential for forming strong metallic bonds during sintering. However, the efficiency of H_2-annealing is dependant on oxide chemistry, which is rarely made of pure/stoichiometric species. The objective here was to perform an in-depth characterization of the oxides found on WA steel particles to understand their behaviour during H_2-annealing. It investigates the relationship between the chemical composition of pre-alloyed steels (Cr, Mn, Mo, Si), the chemical composition of the surface oxides and their modification due to H_2-annealing. Particular attention is given to the impact of the difference between Si(wt.%) and Mn(wt.%) contents on powder oxidation. Characterization was performed using scanning and transmission electron microscopy coupled with energy dispersive X-ray spectroscopy. Characterization before and after annealing provided insights into the dynamics of oxides reduction according to powder chemistry.

Keywords: Water atomization, Steel powder, Surface oxidation, Scanning electron microscopy, Transmission electron microscopy

1. Introduction

Water-atomization (WA) stands out as an efficient way to fabricate chemically homogenous pre-alloyed steel powders. Careful selection of alloying elements allows for the production of powders tailored to meet specific mechanical properties. However, the WA process intrinsically results in highly oxidized powder surfaces due to the reaction between the molten metal and water vapor in the atomization chamber. The types of oxides formed depend on the chemical composition of the liquid metal, particularly chemical elements having a high affinity for oxygen, such as Si, Mn, and Cr. The latter tend to form thermodynamically stable oxide compounds that are challenging to remove via conventional H_2-annealing treatments. Sufficient removal of surface oxide is however required to ensure the formation of strong metallic bonds during sintering.

Previous studies conducted on a few industrial WA steel powders containing Cr and Mn revealed that particle surfaces are mainly covered by an iron oxide layer, along with localized oxides containing Cr, Mn, but also Si (1-3). H_2-annealing treatments have shown good efficacy in reducing iron oxides, but seem limited when it comes to Cr, Mn, and Si-rich oxides. In fact, these stable oxides seem to form during annealing due to the "internal getter effect", an oxygen transfer phenomenon that describes how elements with a high affinity for oxygen can be further oxidized by collecting the oxygen atoms from oxides that are more easily reduced (2). Identifying those highly stable oxides presents challenges as they are not likely pure/simple oxides. Additionally, characterization techniques such as X-ray photoelectron spectroscopy are not ideal for analyzing powder samples. The irregular shape of the WA particles creates a rough surface topography that significantly affects the spectral intensities of photoelectrons, making quantitative measurements difficult to perform.

Previous studies also showed that Si and Mn contents greatly influence the oxygen concentration of WA steel powders, but the mechanism by which these chemical elements affect oxide formation has not been fully investigated (4,5). Herein, this study aims to comprehensively characterize the surface oxides on WA steel particles and their response to H_2-annealing. Using state-of-the-art scanning and transmission electron microscopes (SEM, TEM) coupled with energy dispersive X-ray spectroscopy (EDS), this work aims to establish the relationship between the nominal chemical composition of pre-alloyed steels (Cr, Mn, Mo, Ni, Si), the chemical composition of the surface oxides and their modification induced by H_2-annealing. Specifically, it focuses on the influence of Si and Mn contents on surface oxidation of steel powders during atomization, as well as their response to annealing.

2. Materials & Methodology

To carry out this experiment, 2 pre-alloyed steel powders were produced by WA at the Powder Metallurgy Laboratory of Université Laval and were then sieved to collect the particles in the size range of 106 µm – 150 µm. A portion of the particles collected underwent an annealing treatment performed in a laboratory tube-furnace under a protective atmosphere composed of 90 vol.% argon – 10 vol.% hydrogen (dew point approximately -60 °C). Samples were heated at a rate of 10 °C/min up to 1 000 °C and held at that temperature for 1 h before cooling down to room temperature.

Surface characteristics of powders were first assessed using a JEOL FEG JSM-7600F SEM operated at 5 kV and equipped with an Oxford Instrument X-MaxN EDS detector. This voltage was used to limit the electron/specimen interaction volume when performing EDS analysis on surface oxides. Since the thickness of a given oxide feature cannot be known for certain in SEM, this helped minimize the signal contribution coming from the steel underneath the oxides. For reference, the emission depth of characteristic Fe Lα X-rays is estimated to be around 200nm. SEM results enabled identification of various classes of oxides based on their relative chemical composition and on their morphology.

*corresponding author, E-mail : carl.blais@gmn.ulaval.ca

This paper is licensed under Creative Commons (CC BY-NC-ND). If the further information is needed for this license, please visit the following website, https://creativecommons.org/licenses/by-nc-nd/4.0/deed.en
March, 2025

Table 1 presents the chemical composition of the 2 powder lots in the as-atomized and annealed state. Carbon and oxygen contents were respectively assessed by the combustion method (ELTRA CS- 800), and by the gas fusion method (LECO CS-200). Concentration of Si, Mn, Cr, Ni, and Mo were quantified using a microwave plasma-atomic emission spectrometer (4200 MP-AES, Agilent Technology).

Table 1. Chemical composition of the experimental powders used in this study (wt.%)

	Si	Mn	Cr	Ni	Mo	O (as-atomized)	O (annealed)	C (as-atomized)	C (annealed)	Fe
HighSi	1.2	0.14	0.54	0.85	1.0	0.48	0.20	0.14	0.02	Bal.
LowSi	0.1	0.17	0.31	0.91	1.1	0.51	0.14	0.10	0	Bal.

Regions corresponding to surface oxides were then selected to be characterized by TEM. Thin foils suitable for TEM analysis were produced using a lift-out focus ion beam (FIB) technique with a Helios 5 UX FIB-SEM microscope (ThemoFischer Scientific). Since FIB milling can be damaging to surfaces, a platinum (Pt) protective layer was first deposited using the electron beam on the regions of interest to preserve the surface features of the particles. In some instances, a carbon layer was deposited prior to the Pt layer as an additional protective coating.

TEM characterization was performed using a JEOL JEM-F200 microscope equipped with a cold field emission gun operating at 200 kV. Samples were observed in bright-field mode, as well as in dark-field scanning transmission electron microscopy (STEM) mode. Selected area electron diffraction (SAED) was used to acquire diffraction patterns of specific regions. EDS spectra were acquired using two silicon drift EDS detectors (JEOL). Images were captured using a Gatan OneView camera and Gatan DigitalMicrograph software. Note that copper (Cu) and Pt were excluded from all quantifications as those signals come from the Cu grid and the Pt deposition.

3. Results and discussion

3.1 Oxygen content

Fig. 1 shows the oxygen content for both powders before and after annealing, as well as the difference between their Si and Mn content. Previous studies on S7 tool steel powders and 304L stainless steel powders indicated that a greater difference Si (wt. %) – Mn (wt %) results in a lower oxygen content in as-atomized powders (4-5). Here, LowSi and HighSi powders have a similar oxygen content (0.51 wt.%, and 0.48 wt.%, respectively) in their as-atomized state despite having a significant difference in their Si (wt. %) – Mn (wt %) value. After annealing, LowSi powder has the lowest oxygen content (0.14 wt.%), even if it had the highest oxygen content in its as-atomized state. While this trend goes against previous findings, more powders with different Si (wt. %) – Mn (wt. %) need to be studied to fully understand the effect of those alloying elements on WA powder oxidation.

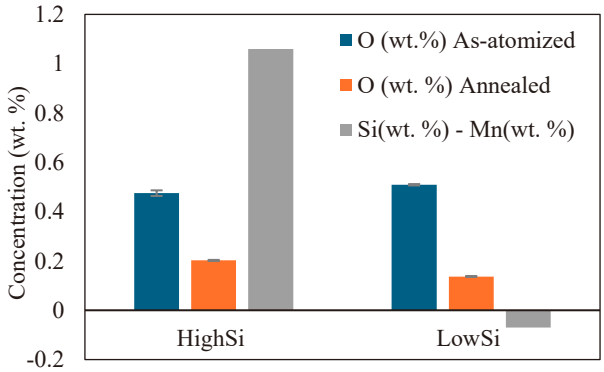

Fig. 1. Effect of Si and Mn concentrations on the oxygen content of WA steel powders in the as-atomized state.

3.2 SEM and EDS

Surface morphology and composition of the 2 experimental powders produced were first assessed by SEM imaging and EDS. Fig. 2 showcases SEM micrographs of typical particles from both powders in their as-atomized condition as well as after annealing. At first glance, it is possible to see that as-atomized particles are almost fully covered by oxides. SEM-EDS analysis presented in Fig. 3 reveals that LowSi particles (Fig.2a) are covered by a smooth, but discontinued Fe oxide layer, while HighSi particles are covered by Si/Mn-rich oxides (Fig.2c – red arrows) in addition to the Fe oxide layer (Fig.2c – yellow arrow). Si/Mn-rich oxides form distinct, patch-like areas at the surface of the particles that can significantly vary in size. Although the selected HighSi particle is deemed as "typical", is it important to note there is significant heterogeneity within a powder lot. This means that some particles analyzed exhibited complete coverage by Si/Mn-rich oxides, while other displayed numerous patches, or a singular patch, etc.

After annealing, both powders showed no trace of "pure" Fe oxides. This could be foreseen, as Fe oxides are readily reducible at around 400 °C degrees in a hydrogen containing atmosphere (2). Although one might have expected annealed LowSi particles to be oxide-free, this is not what is observed. While most of the surface of the particle shown is metallic Fe (Fig.2b – black arrow), some oxidized regions enriched in Si, Mn and Cr are present (Fig.2b – red arrow). Since these types of oxides were absent in the as-atomized state of the LowSi powders, they were formed during the annealing process via the "internal getter effect": reduction of Fe oxides released oxygen, which created a local oxidizing

atmosphere for elements with a high affinity for oxygen like Si, Mn and Cr (2). This phenomenon is less noticeable in the HighSi SEM micrographs since particles already exhibited Si/Mn-rich oxides in their as-atomized state. The morphology of the oxide patches in the annealed state appears similar for both powders, as depicted in Fig. 3. Within the patches, there are several nanometer-sized circular regions that seem to have undergone reduction (Fig.3b-d – red arrows). Beside the "patch"-like morphology, HighSi particles also exhibit thin regions composed of Si-rich oxides that formed at grain boundaries (Fig.3d. eds9).

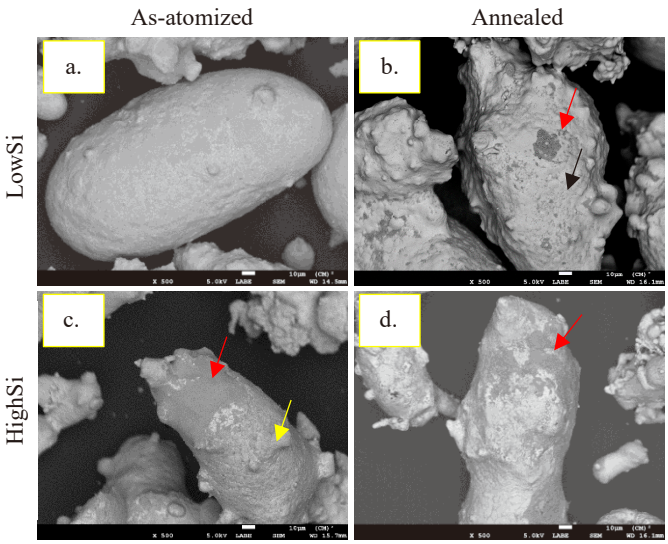

Fig 2. SEM micrographs of typical particles found in LowSi and HighSi powder lots in both the as-atomized and annealed state. See text for explanations related to the use of arrows.

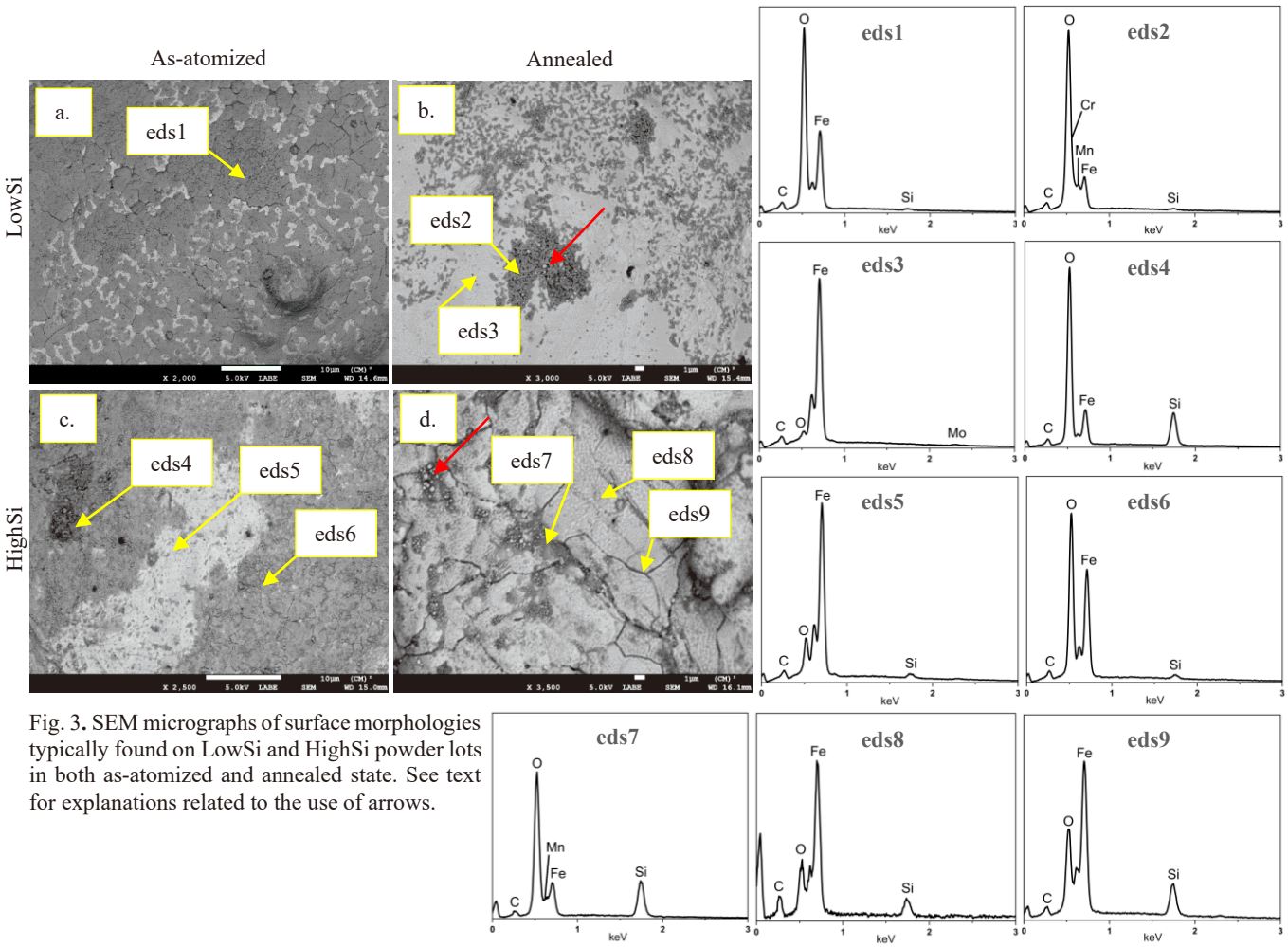

Fig. 3. SEM micrographs of surface morphologies typically found on LowSi and HighSi powder lots in both as-atomized and annealed state. See text for explanations related to the use of arrows.

3.3 TEM and EDS

To gain insights into the Si/Mn/Cr-rich oxide patches that can withstand the annealing process, thin foils were prepared for TEM analysis. First, Fig. 4a shows a bright field TEM image of a thin foil extracted from an as-atomized HighSi oxide patch. The thickness of the oxidized area shown is variable but can go as high as ~3µm. Analysis of the EDS spectra performed with Gatan DigitalMicrograph software indicated that there are 3 main phases/features with distinct morphologies: i) a "background" oxide ii) a diffuse network oxide iii) a spherulite-like oxide. Fig. 4b shows those 3 features at higher magnifications. The predominant "background" phase appears to be a mixed Fe/Si-rich oxide that is amorphous (Fig. 4b. eds1). Next, the diffuse network phase has a Si/O stoichiometry that is consistent with SiO_4 (Fig. 4b. eds2). This network extends throughout the oxidized region, and a similar phase is also observed near the metal/oxide interface (Fig. 4c. eds3). However, EDS analysis suggests that the Si-rich oxide present at the interface is SiO_3 rather than SiO_4. Note that the dotted pattern at the metal/oxide interface corresponds to Pt redeposition during FIB milling. Lastly, the spherulites scattered across the oxidized region exhibit a very fine structure. A high-resolution TEM micrograph shown in Fig. 4d suggests that it is comprised of 2 oxide phases, one phase with higher Si content, and one phase with higher Cr and Fe content. The entire spherulite may seem crystalline, but it is conceivable that only the Fe/Cr-rich phase is, while the Si-rich phase remains amorphous. The diffraction pattern shown in Fig. 4b can be indexed as a face-centered cubic crystal that could correspond to $FeCr_2O_4$. Since the 2 phases overlap in the thickness of the thin foil, it is difficult to determine their exact chemical composition.

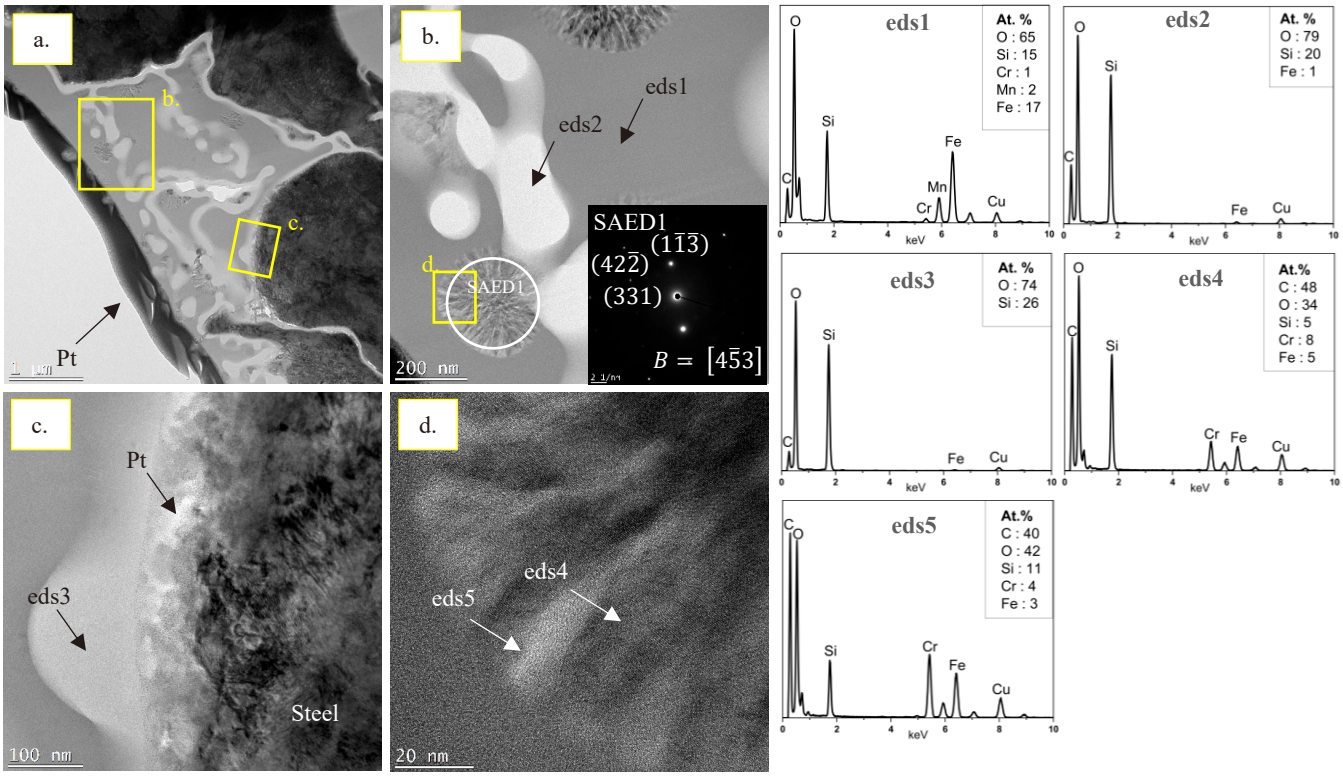

Fig. 4. a) Bright-field TEM micrograph showing the thin foil sampled from the surface of an as-atomized HighSi particle. Pt indicates the surface of the particle. b) Higher magnification micrograph showing the 3 main features observed within the oxidized region and diffraction pattern of the spherulite. c) Higher magnification micrograph showing the metal/oxide interface. d) High-resolution micrograph showing the 2 phases of the spherulite feature identified in b. Carbon is excluded from EDS quantification, except for eds4, and eds5.

Fig. 5a shows TEM micrographs of a specimen extracted from an annealed HighSi oxide patch. Annealing induced noticeable changes in the morphology and composition of the oxide patches. The diffuse SiO_4 network found in the as-atomized lamella appears to have transformed into a phase consistent with SiO_3 in response to H_2-annealing. It seems like this SiO_3 oxide phase retracted, coalescing into one prominent circular feature, as shown in Fig. 5b. The 'background' phase in the annealed specimen appears to be composed of crystalline Si/Mn-rich oxides (Fig. 5c. eds6), in contrast to the amorphous Fe/Si oxides present in the as-atomized sample. In fact, Fe seems less prevalent in the oxides observed in the annealed state. This may be the result of the "internal getter effect": most of the mixed Fe/Cr/Si/Mn oxides transformed into more thermodynamically stable Cr/Si/Mn oxides during annealing. Fe-rich oxides that remain form distinct areas (Fig. 5c. eds7). The metal/oxide interface in the annealed sample exhibits oxides with diverse compositions and shapes, contrasting with the homogeneity observed in the as-atomized state. Here, distinct phases are noticeable: crystalline polygon-shaped oxides that are enriched in Si and Cr (Fig. 5e. eds9), round-shaped oxides that are enriched in Fe, Si and Mn (Fig. 5c. eds8), and an amorphous Si-rich phase that appears to be SiO_3 (Fig. 5c. eds5). The annealing process seemingly facilitated the segregation, coalescence, and in certain cases, crystallization of phases initially present at the interface. Spherulites previously observed are still present in this sample, but their two-phase structure is much coarser and is basically free from Fe (Fig. 5b. eds3, eds4). High-resolution imaging shows that the 2 phases of the annealed spherulites seem to be made of crystalline Cr-rich oxides and amorphous Si-rich oxides (Fig. 5d). Again, it is difficult to analyze both phases separately as they overlap in the thickness of the thin foil.

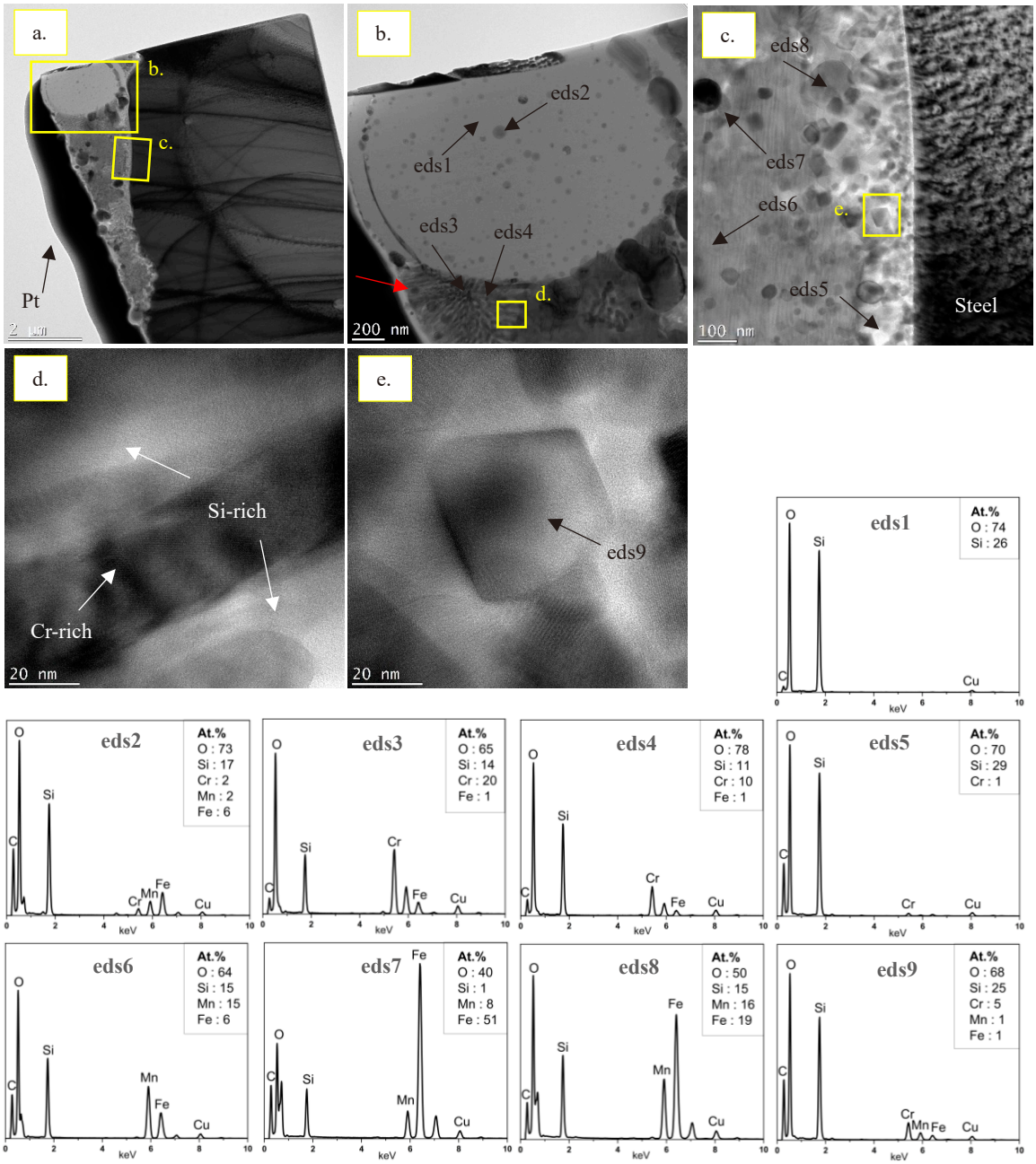

Fig.5. a) Bright-field TEM micrograph showing the thin foil sampled from the surface of an annealed HighSi particle. Pt indicates the surface of the particle. b) Higher magnification micrograph showing the SiO_3 phase, and a spherulite (red arrow). c) Higher magnification micrograph showing the metal/oxide interface. d) High-resolution micrograph showing the 2 phases of the spherulite features identified in b. e) High-resolution micrograph showing a polygon-shaped oxide identified in c. Carbon was excluded from EDS quantification.

Fig. 6 shows TEM micrographs of a specimen extracted from the Fe oxide layer that covers most of the as-atomized LowSi particles. The first point to notice is the uniform thickness of the oxide layer, typically ranging from 100 nm to 250 nm, which contrasts the thick oxide patches present in the as-atomized HighSi sample. Despite the results obtained from SEM-EDS analysis, the oxide layer is not solely composed of Fe oxides. In fact, it seems like it is a crystalline bilayer, where the outermost layer is Fe oxides (Fig. 6b. eds1), and the innermost layer is mixed Fe/Cr-rich oxides (Fig. 6b. eds2). Cr seems to be the only alloying element that was significantly oxidized during atomization. Fig. 7a shows TEM micrographs of a specimen extracted from an oxide patch found on an annealed LowSi particle. The rather uniform oxide bilayer transformed into oxide "aggregates", which form a porous structure. This reorganization of the uniform bilayer could have been promoted by the presence of Fe oxides. Since the reduction of Fe_2O_3 typically leads to the formation of porous products (6), the reduction of the outer Fe oxides possibly formed pores that allowed H_2 to penetrate the layers. Note that, because of the porosity, carbon and Pt were able to infiltrate the oxide patch during the preparation of the thin foil. Numerous regions scattered in the oxide aggregates seem to have undergone effective reduction during annealing (Fig7b. eds1). The diffraction pattern shown in Fig. 7b can be indexed as a body-centered cubic crystal (BCC) which is consistent with ferrite. The oxides that withstood annealing or that were formed during the process are mainly enriched in Cr and Mn (Fig7b. eds2). This is different from what was observed in the HighSi samples. In fact, it seems that a higher Si content promotes the formation of Si-rich or Si/Mn-rich oxides over Cr/Mn-rich oxides. Conversely, when Si content is lower, it does not seem to be preferentially oxidized.

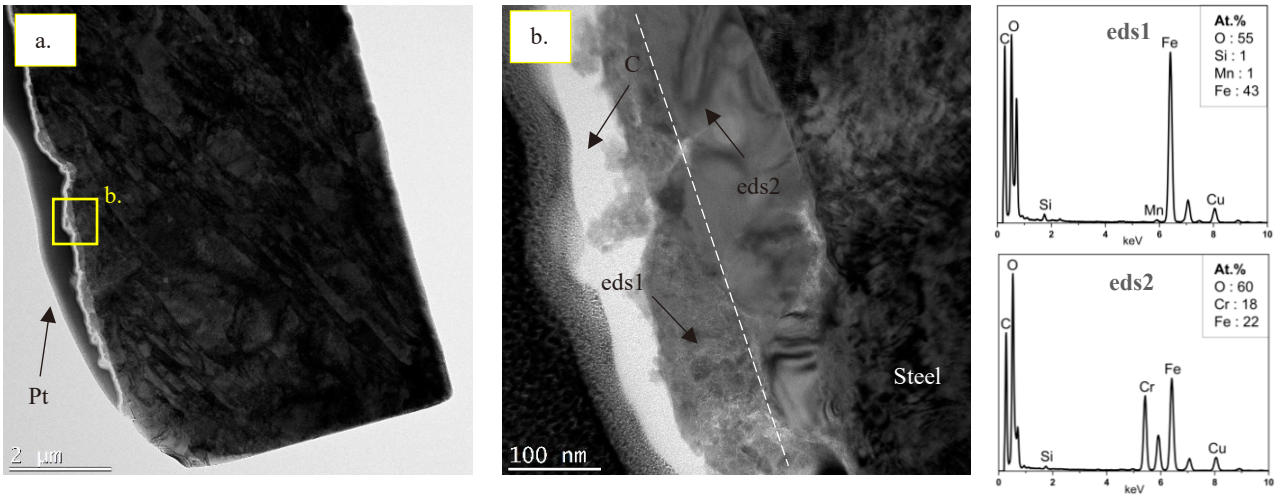

Fig. 6. a) Bright-field TEM micrograph showing the thin foil sampled from the surface of an as-atomized LowSi particle. Pt indicates the surface of the particle. b) Higher magnification micrograph showing the oxide bilayer. Dotted line emphasizes the separation between the 2 layers. A carbon layer is present on top of the bilayer due to the sample preparation process. Carbon was excluded from EDS quantification.

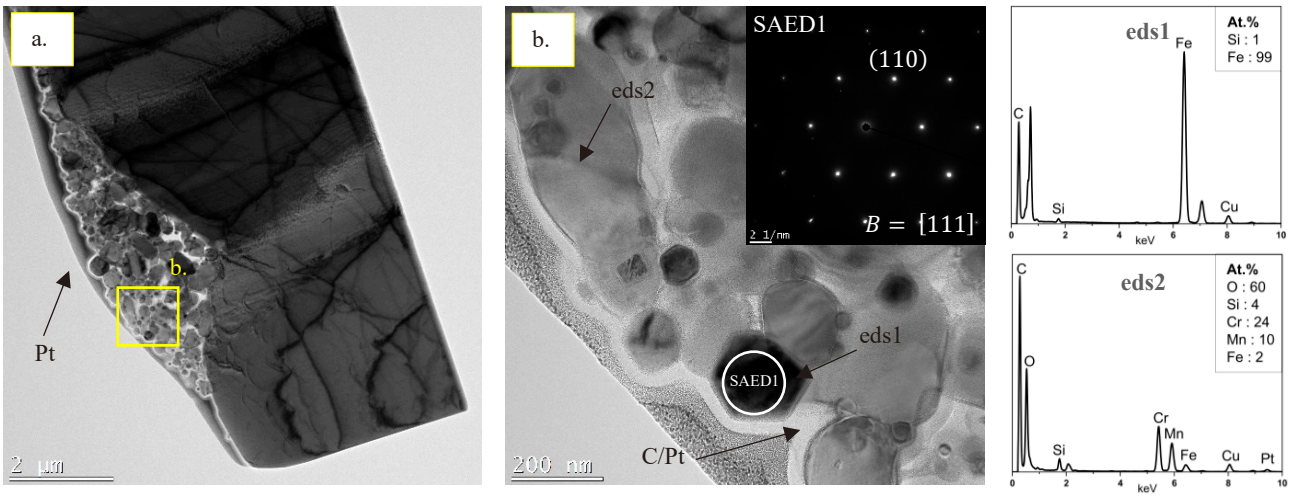

Fig. 7. a) Bright-field TEM micrograph showing the thin foil sampled from the surface of an annealed LowSi particle. Pt indicates the surface of the particle. b) Higher magnification micrograph showing the porous structure made of oxides and metallic Fe. Diffraction pattern corresponds to ferrite. Carbon was excluded from EDS quantification.

4. Conclusion

The aim of this work was to characterize the surface oxides on WA steel particles and their response to H_2-annealing. SEM/EDS and TEM/EDS were used to analyze powders in their as-atomized and annealed state. Table 2 provides a summary of the key observations. Here are the main takeaways:

i) Results show that the oxygen content of as-atomized HighSi and LowSi powders is similar. The difference Si (wt. %) – Mn (wt. %) did not influence the as-atomized oxygen content, contrary to what has been reported in the literature. However, more work is needed to understand the effect of those alloying elements on WA powder oxidation.

ii) SEM/EDS analysis enabled the identification of the main chemical classes of oxides present, namely "pure" Fe oxides, and mixed Fe/Si/Cr/Mn oxides. Fe oxides form a uniform layer on as-atomized particles, whereas mixed oxides appear as patches, or networks at grain boundaries on as-atomized and/or annealed particles.

iii) TEM/EDS analysis revealed the oxides patches form thick structures that are complex and heterogenous. High-resolution imaging showed multiple types of oxides, including spherulites, networks, spheres, and polygons, all with different chemical compositions.

iv) H_2-annealing successfully reduced pure Fe oxides but did not eliminate mixed Fe/Si/Mn/Cr oxides. In fact, annealing conditions promoted the formation of more thermodynamically stable oxides through a phenomenon known as the "internal getter effect".

v) HighSi powder contains more Si-rich oxides, while LowSi powder contains more Cr/Mn-rich oxides. Si content influences the type of oxide that is formed during atomization.

This study contributes to a broader effort to enhance our understanding of oxide behaviour during annealing. Further research is needed to determine the details of the mechanisms responsible for the transformation of oxides from their as-atomized state to their annealed state.

Table 2. Summary of the phases observed in both HighSi and LowSi powders in their as-atomized and annealed state

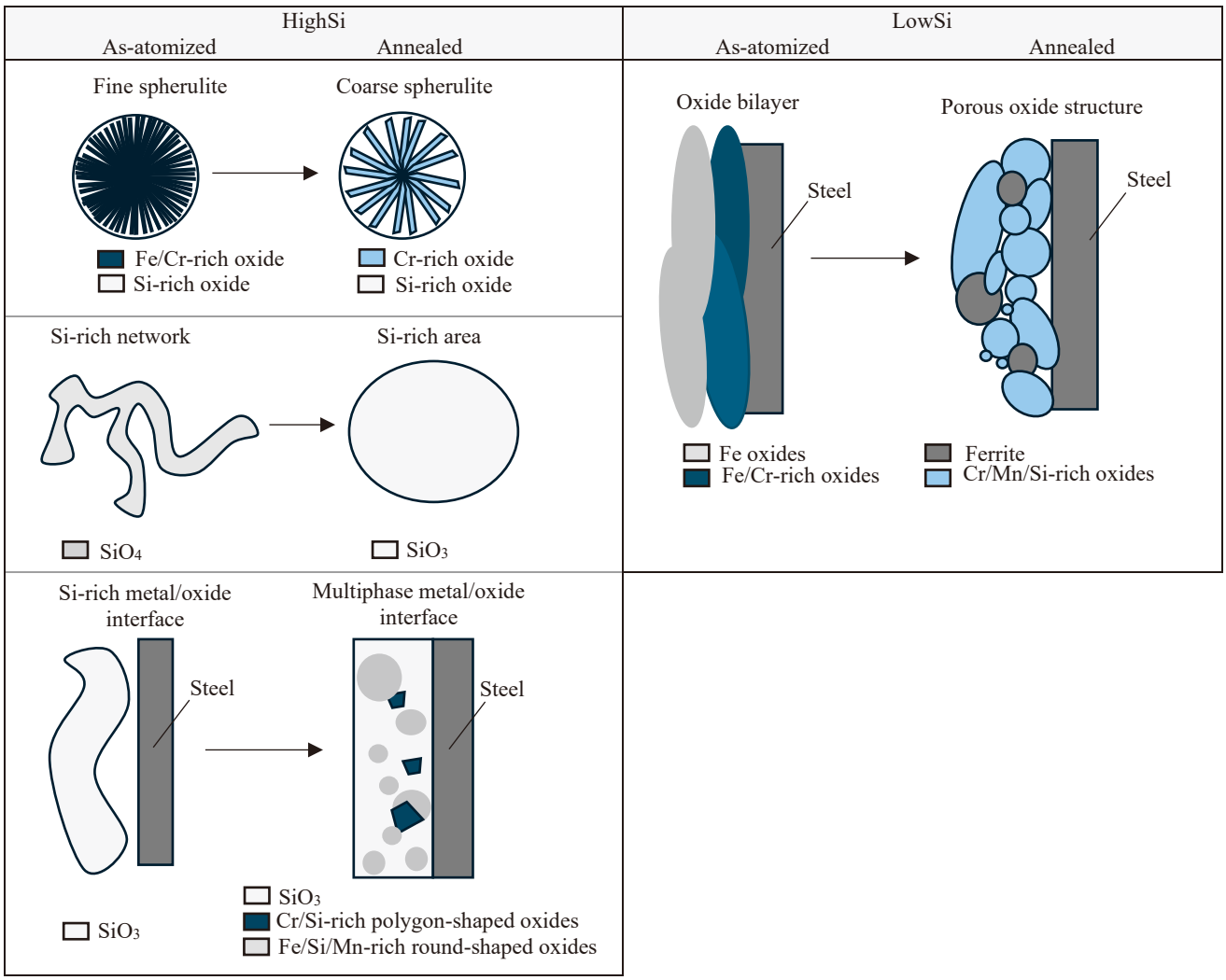

5. Acknowledgements

The authors thank the Natural Sciences and Engineering Research Council of Canada (NSERC) as well as the Fonds de recherche du Québec Nature and Technology (FRQNT) for their financial support.

6. References

1) J. WENDEL, R. SHVAB, R.CAO, E. HRYHA, L. NYBORG, Surf. Interface Anal., **50**(2018) 1065-1071.
2) C. GIERL-MAYER, R.D. CALDERON, H. DANNINGER, Jom, **68**(2016) 920-927.
3) D. CHASOGLOU, E. HRYHA, M. NORELL, L. NYBORG, Appl. Surf. Sci., **268**(2013) 496-506.
4) W.F. WANG, Powder Metall., **37**(1994) 33-36.
5) D. MUTEL, Développement de poudres d'acier à outils S7 par atomisation à l'eau pour la fabrication additive par fusion laser sur lit de poudre (LPBF) [Thesis], Université Laval(2023).
6) D. SPREITZER, J. SCHENK, Steel Res. Int., **90**(2019) 17.

Received June 30, 2024; Revised June 30, 2024; Accepted August 20, 2024